JOURNAL OF SPACECRAFT AND ROCKETS
Vol. 47, No. 2, March–April 2010

Determination of Center-of-Mass of Gravity Recovery and Climate Experiment Satellites

Furun Wang,* Srinivas Bettadpur,† and Himanshu Save‡
University of Texas at Austin, Austin, Texas 78759
and
Gerhard Kruizinga§
Jet Propulsion Laboratory, California Institute of Technology, Pasadena, California 91109

DOI: 10.2514/1.46086

The Gravity Recovery and Climate Experiment (GRACE) mission, launched on 17 March 2002, uses radiometric tracking between twin, coorbiting satellites in a polar 500-km-alt orbit, in order to make detailed measurements of Earth's gravity field. These measurements have led to significant, new insights into climate-driven mass transport in the Earth system. A key element of the GRACE scientific measurement suite is the high-precision accelerometer required to measure the nongravitational accelerations acting on the GRACE satellites. To avoid contamination of nongravitational acceleration measurements, the GRACE mission requires the proof mass of the accelerometer to be positioned within 100 μm (0.1 mm) of the center-of-mass of satellite. This is accomplished using a dedicated center-of-mass calibration maneuver every few months. This paper describes the GRACE center-of-mass calibration maneuver design and implementation details and presents the data analysis used to routinely measure the center-of-mass offset. Using external validation and internal consistency checks, we show that the GRACE satellite center-of-mass offset is being measured routinely to approximately 25 to 40 μm precision along the three satellite axes.

Nomenclature

$\mathbf{a}_{\mathrm{exc}}$	=	accelerometer excitations or input linear accelerations, $\mathrm{m/s^2}$
$\mathbf{a}_{\mathrm{ng}}$	=	nongravitational acceleration vector, $\mathrm{m/s^2}$
$\mathbf{a}_{\mathrm{gg}}$	=	gravity-gradient acceleration vector, $\mathrm{m/s^2}$
$\mathbf{a}_{\mathrm{thr}}$	=	thrust acceleration vector, $\mathrm{m/s^2}$
$\mathbf{B}(t)$	=	Earth's magnetic field vector
$\mathbf{b}(t)$	=	time-dependent accelerometer drift vector, $\mathrm{m/s^2}$
$\mathbf{d}$, $\dot{\mathbf{d}}$, $\ddot{\mathbf{d}}$	=	center-of-mass offset vector and its time derivatives in satellite reference frame
f	=	frequency, Hz
J	=	satellite moment-of-inertia matrix
$\mathbf{m}(t)$	=	magnetic moment vector, $\mathrm{Am^2}$
$\mathbf{n}(t)$, $\boldsymbol{\eta}(t)$	=	vectors representing accelerometer measurement noise, $\mathrm{m/s^2}$
$\mathbf{q}$, $\dot{\mathbf{q}}$	=	attitude quaternion and its time derivative in satellite reference frame, nondimensional
$S(t)$	=	time-dependent scale matrix of the accelerometer, nondimensional
$\mathbf{T}(t)$	=	torque acting on satellite, nm
t	=	time, independent variable, s
x, y, z	=	scalar components along satellite reference frame
$\boldsymbol{\alpha}$	=	slope vector in accelerometer adjustment model, $\mathrm{nm/s^2}$ per s
$\boldsymbol{\beta}$	=	intercept vector in accelerometer adjustment model, $\mathrm{nm/s^2}$
$\boldsymbol{\omega}$	=	angular velocity vector, rad/s
$\dot{\boldsymbol{\omega}}$	=	acceleration vector, $\mathrm{rad/s^2}$

I. Introduction

THE joint U.S. (NASA) and German (DLR, German Aerospace Research Center) Gravity Recovery and Climate Experiment (GRACE) mission was launched on 17 March 2002, with the goal of providing accurate high-resolution measurements of the time-variable and long-term mean mass distribution within the Earth system [1,2]. The GRACE mission provides estimates of mass flux through the observation of its effect on the variations in the Earth's external gravity field by making continuous measurements of relative orbital motion between the twin GRACE satellites. The distance between the two GRACE satellites, which were launched into a 480-km-alt polar orbit and separated by approximately 200 km in the flight direction, is measured using a precise K-band microwave ranging system [3]. The influence of nongravitational accelerations on the intersatellite distance measurement is removed in data processing, using measurements from the SuperSTAR accelerometer [4].

The SuperSTAR accelerometer uses electrostatic suspension of a proof mass within an electrode cage in order to sense the relative linear and angular accelerations between the cage and the proof mass. The electrode cage, through the accelerometer sensor-unit assembly, is rigidly attached to the GRACE spacecraft. While gravitational accelerations affect both the accelerometer proof mass and the spacecraft, nongravitational forces affect only the spacecraft, so that the relative accelerations between the electrode cage and the proof mass are a measurement of the nongravitational accelerations acting on the spacecraft. The SuperSTAR instrument provides measurements of both linear nongravitational and total angular accelerations of the spacecraft.

If the center of the proof mass of the accelerometer is not located at the center of mass (CM) of the entire spacecraft, the accelerometer senses additional accelerations due to the satellite angular motion and the gravity gradients. The offset vector from the origin of the proof mass to the satellite center of mass is referred to as the center-of-mass offset (CM-offset) in this paper. Extensive prelaunch simulations were carried out to assess the impact of this coupling between the CM-offset and simulated satellite angular motion, their impact on the accelerometer output, and its consequent effect on the

Received 23 June 2009; revision received 9 February 2010; accepted for publication 8 February 2010.

*Research Engineer, Center for Space Research, 3925 West Braker Lane, Suite 200.

†Senior Research Scientist, Center for Space Research, 3925 West Braker Lane, Suite 200. Senior Member AIAA.

‡Graduate Research Assistant, Center for Space Research, 3925 West Braker Lane, Suite 200.

§4800 Oak Grove Drive, Mail Stop 301-276.

recovery of the gravity field. Based on the results of these simulations, the GRACE mission required this CM-offset to be less than 100 μm in each component along the satellite body axes.

The GRACE mission has elected to minimize the influence of these centrifugal, tangential, and gravity-gradient accelerations on the accelerometer output by using a strategy of actively measuring and controlling the CM-offset. A center-of-mass calibration (CM-cal) maneuver was designed [5] for the purpose of measuring the CM-offset. The CM-cal maneuver consists of a periodic angular acceleration imposed on the spacecraft using magnetic torquers. The period of the oscillation is chosen such that there is no expectation of any natural variations in the linear accelerations acting upon the satellite at that frequency. If there is any significant CM-offset, the coupling to rotational motion of the satellite induces an oscillatory linear acceleration output from the accelerometer at the same frequency. A regression, therefore, between the linear and angular acceleration output of the SuperSTAR accelerometer during the period of the CM-cal maneuver provides an estimate of the CM-offset.

The outcome of the CM-cal maneuver is an estimate of the CM-offset vector in the satellite body frame. If the offset is larger than a specified limit, a center-of-mass trim (CM-trim) mechanism is used to move the satellite CM relative to the accelerometer proof mass so that the CM-offset is again close to zero. The CM-trim mechanism consists of a mass on spindle, driven by a stepper motor. Shifting the mass on the spindle provides the ability to move the CM of the satellite.

In the GRACE mission, the CM-offset is nonzero due to two reasons. One reason for the offset is the limitations of prelaunch assembly and balancing. Results from the first postlaunch CM-cal experiment suggested that prelaunch balancing had reduced the CM-offset to less than 300 μm. This initial offset was further reduced using a CM-trim almost immediately after launch. Since then, the only reason for a drift in the CM-offset is the differential consumption of the cold-gas (GN2) fuel (used for GRACE attitude and orbit maintenance [6]) from the twin fuel tanks on each satellite. Since the twin fuel tanks are symmetrically placed (fore and aft) relative to the satellite CM in the satellite *X* (or the in-flight) direction, this postlaunch drift manifests itself mainly in the *X* component of the CM-offset. A cutout view (Fig. 1) of the GRACE spacecraft shows the location of the SuperSTAR accelerometer (labeled ACC), the two spherical fuel tanks, and the definition of the satellite-fixed axes, which have their origin at the center of the proof mass of the accelerometer.

The *X* component of the CM-offset estimate, determined using the CM-cal maneuver, is verified against a model of the CM-offset drift based on telemetry of the pressure and temperature of the cold-gas fuel onboard the satellites. This model-based prediction of the CM-offset drift is also used as a tool to schedule the CM-cal maneuvers, which are typically being carried out every three to six months. The CM-trim mechanism has been used seven times during the course of the mission so far (between March 2002 and August 2008) to reduce the CM-offset close to zero. Table 1 presents a summary of the requirements and capabilities for the measurement and control of the CM-offset.

In this paper, we discuss the design of the CM-cal maneuvers during the course of the GRACE mission. We then present the sample data from CM-cal maneuvers, the algorithms for the analysis of this data, and an assessment of the accuracy of the determination of the CM-offset.

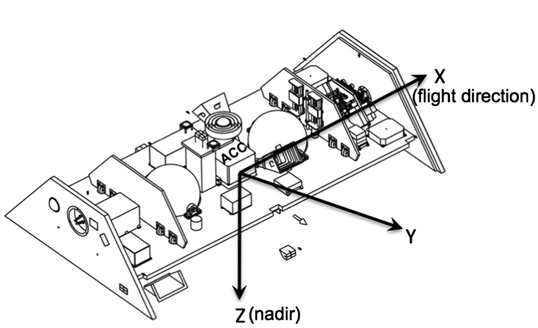

Fig. 1 Cutout view of one of the GRACE satellites.

Table 1 Summary of CM-offset measurement requirements and trim capabilities for the GRACE mission

CM-offset requirement	<0.1 mm in each direction
CM-cal maneuver	
Oscillation period	12 s
Directions	Separately in roll, pitch, and yaw
Experiment duration	180 s
CM-trim capabilities[a]	
Trim mass	Twin 4.8 kg masses on each axis
Maximum travel distance of trim mass	±100 mm
CM control capability	±2 mm

[a]Nominal satellite mass is 485 kg.

II. CM Calibration Maneuver

The relative acceleration between the accelerometer proof mass and the electrode cage (or the excitation) of the SuperSTAR accelerometer can be written as

$$\mathbf{a}_{\text{exc}} = -\ddot{\mathbf{d}} - \dot{\boldsymbol{\omega}} \times \mathbf{d} - 2\boldsymbol{\omega} \times \dot{\mathbf{d}} - \boldsymbol{\omega} \times (\boldsymbol{\omega} \times \mathbf{d}) + \mathbf{a}_{\text{gg}} + \mathbf{a}_{\text{ng}} + \mathbf{a}_{\text{thr}} \tag{1}$$

where the principal quantities of interest are $\mathbf{a}_{\text{ng}}$, the nongravitational accelerations acting upon the satellite and $\mathbf{a}_{\text{thr}}$, the residual rectilinear acceleration on the spacecraft due to imperfectly coupled attitude-control thrusters. Both of these influence the evolution of the trajectory of the spacecraft and are of interest in the analysis of the intersatellite ranging measurements. The remaining terms do not influence the orbit and are thus desired to be close to zero. In Eq. (1), $\mathbf{d}$ is the CM-offset, which is a vector from the proof-mass origin to the CM of the satellite, and $\dot{\mathbf{d}}$ and $\ddot{\mathbf{d}}$ are its first and second time derivatives relative to the satellite body-fixed system. The spacecraft's instantaneous angular velocity with respect to the inertial system is $\boldsymbol{\omega}$, and the spacecraft's instantaneous angular acceleration is $\dot{\boldsymbol{\omega}}$. Finally, $\mathbf{a}_{\text{gg}}$ is the acceleration due to gravity gradients. The goal of the CM-cal maneuver is to estimate $\mathbf{d}$ in the satellite frame. The purpose of the CM-trim is to drive this offset close to zero, such that the rotational and gravity-gradient terms in Eq. (1) are negligible.

The accelerometer data output vector may be written as

$$\mathbf{A}_{\text{out}} = \mathbf{b}(t) + S(t) \cdot \mathbf{a}_{\text{exc}} + \mathbf{n}(t) \tag{2}$$

where $\mathbf{b}$ represents the vector of a signal-independent, time-variable instrument drift, $S(t)$ is a 3×3 diagonal matrix with the potentially time-varying scales along its diagonals, and $\mathbf{n}(t)$ represents measurement noise vector. Instrument analysis has shown that offdiagonal scale coupling terms or quadratic terms in the signal are negligible.

A. Maneuver Design

From the SuperSTAR accelerometer, we have measurements of the linear acceleration $\mathbf{A}_{\text{out}}$, as well as the angular acceleration $\dot{\boldsymbol{\omega}}$. The essence of the CM-cal maneuver [5] is to introduce an oscillatory variation in $\dot{\boldsymbol{\omega}}$ that is unique and different from expected variations in the last three terms in Eq. (1). In the presence of an offset $\mathbf{d}$, the accelerometer output $\mathbf{A}_{\text{out}}$ contains the same oscillatory signal, and a regression between measurements $\mathbf{A}_{\text{out}}$ and $\dot{\boldsymbol{\omega}}$ allows the estimation of $\mathbf{d}$.

For the GRACE mission, the period of the angular oscillations was chosen to be 12 s, with one maneuver consisting of 15 such oscillations about each satellite-fixed axis, lasting for a total of 180 s [5]. A complete CM-cal campaign consists of two such maneuvers in each of the satellite-fixed roll, pitch, and yaw directions. Together with associated satellite control, housekeeping, and ground monitoring activities, a complete CM-cal campaign lasts approximately 8 to 12 h.

It is reasonable to assume that the CM-offset is stable (or constant) in the relatively short duration (one day) of one complete CM-cal campaign. The GRACE attitude-control system is designed to meet the requirement that within each 180 s CM-cal maneuver, there must be no attitude-control thruster firings. These conditions are imposed to ensure that the terms including $\dot{\mathbf{d}}$ and $\ddot{\mathbf{d}}$ in Eq. (1) are negligible.

Within each CM-cal maneuver, there are small variations in the nongravitational accelerations, due to the approximately 1250 km traverse through the atmosphere and due to small variations in the satellite area presented to the relative wind in this 180 s duration. However, we may expect the resulting variations to be slowly changing; in particular, we do not expect the variations to have the nearly 12 s characteristic period of the regular angular motions. The gravity-gradient term, dominated largely by the change of satellite radius over this time span, is also expected to be slowly changing.

As a result of this maneuver design, the unique angular oscillation at the 12 s period is matched by a corresponding oscillatory linear acceleration that is output from the SuperSTAR accelerometer in proportion to the CM-offset. The angular oscillations are imposed on the GRACE satellites using a magneto-torquer system, which consists of three magnetic torque rods (one along each satellite axis) and the associated drive electronics. Each of the three rods consists of a cylindrical core and two coils. The axis of the coil is the same as the cylinder axis of the magnetic core. Each magneto-torquer is aligned parallel to one satellite axis.

The magnetic torque rods are electromagnets generating a dipole moment $\mathbf{m}$ that when interacting with the Earth's magnetic field $\mathbf{B}$ produces a torque $\mathbf{T}$ according to the vector product formula $\mathbf{T} = \mathbf{m} \times \mathbf{B}$. The total magnetic dipole moment $\mathbf{m}$ is given by vector superposition of the three individual dipole moments. Any direction of $\mathbf{m}$ can be established using at least three magnetic rods such that the rods' longitudinal axes mark an orthogonal coordinate frame. The magnetic torque rods on the GRACE satellites have dipole moments ranging from -30 to $+30$ Am^2 and are mounted parallel to the satellite axes within an alignment error of 0.06 deg. There are several schemes for activating the magnetic moment along each axis to generate the total moment. In the GRACE mission, the expected torque $\mathbf{T}_e$ is commanded, and the attitude-control system software calculates the magnetic moment to be activated such that

$$\mathbf{m} = k\mathbf{M}_e \tag{3}$$

where $\mathbf{M}_e$ is equal to $\mathbf{B} \times \mathbf{T}_e$, and k is equal to $M_A/M_{\max}$. The Earth's magnetic field $\mathbf{B}$ is obtained from a magnetic field model. $\mathbf{M}_A$ is the maximum saturation momentum, which is 30 Am^2 for the GRACE mission. $M_{\max}$ is the maximum absolute value of components of $\mathbf{M}_e$.

In each calibration maneuver, the expected magnetic torque is commanded along only one satellite axis and it is always very large in order to ensure that the magnetic moment is saturated at least along one axis. For example, when the expected torque is commanded along the roll axis, $\mathbf{T}_e$ will be a product of $[1 \quad 0 \quad 0]^T$ $\mathrm{N \cdot m}$ and a standard square waveform function with the desired oscillation period. Conventionally, the maneuvers with the commanded expected torque along the roll, pitch, and yaw axes are called the roll maneuver, pitch maneuver, and yaw maneuver, respectively. Other strategies to activate the magnetic moment are possible, as discussed in [7].

B. Location of CM-Cal Maneuvers

The geographic location of the CM-cal maneuver is governed by three main considerations. The first is the desire to maximize the magnitude of angular acceleration along each axis, since this maximizes the signal for regression, thus improving the calibration accuracy. The magnetic torque is proportional to the Earth's magnetic field, which changes with location, and so the angular velocity and angular acceleration will be quite different with respect to different geographic locations even if the same magnetic moments are activated.

For each maneuver type, angular accelerations result along all three spacecraft axes, though the largest accelerations are in the direction of the maneuver. The total angular acceleration magnitude can be easily predicted for each location, based on $\mathbf{T}_e$, a model for $\mathbf{B}$, and the values of the satellite moments of inertia. The geographic distribution of the absolute values of the angular acceleration vector components in the satellite-fixed frame for each maneuver is plotted in Figs. 2–4.

All angular accelerations in Figs. 2–4 are in the unit of $\mu\mathrm{rad/s}^2$. From the figures, it can be seen that the roll maneuver results in large acceleration along the roll axis over the polar regions, with a magnitude of nearly 20 $\mu\mathrm{rad/s}^2$, but leads to a small acceleration over the equatorial region. The pitch maneuver drives the acceleration along the pitch axis almost in the same magnitude over all regions. There are two near equatorial regions of interest for pitch and yaw maneuvers: one is a pitch maneuver within latitude bounds -20 and $+20°$ and longitude bounds 305 and 325°, which provides large accelerations along both roll and pitch axes, and the other is a yaw maneuver within latitude bounds -20 and $+20°$ and longitude bounds 80 and 140°, which provides a large acceleration along the yaw axis. The largest angular accelerations along roll, pitch, and yaw axes are as high as 20, 4, and 2 $\mu\mathrm{rad/s}^2$, respectively. The magnitude differences along the three axes arise from the orientation of the GRACE spacecraft's flight direction with respect to the Earth's magnetic field and different moments of inertia along each axis.

A second consideration in the selection of maneuver location is to minimize the incidence of signals called *twangs* in the linear acceleration output. Twangs refer to short-lived damped oscillations that can reach up to 30 $\mu\mathrm{m/s}^2$, last from 3 to 10 s, appear almost always in the radial direction measurement, and are believed to be caused by structural vibrations in the GRACE spacecraft [8]. It has been found [8] that the twangs are correlated with geolocation and the sun illumination. Generally (though not without exception), in the near-equatorial regions, fewer twangs have been found when the satellites are in the Earth's shadow. At the higher latitudes, fewer

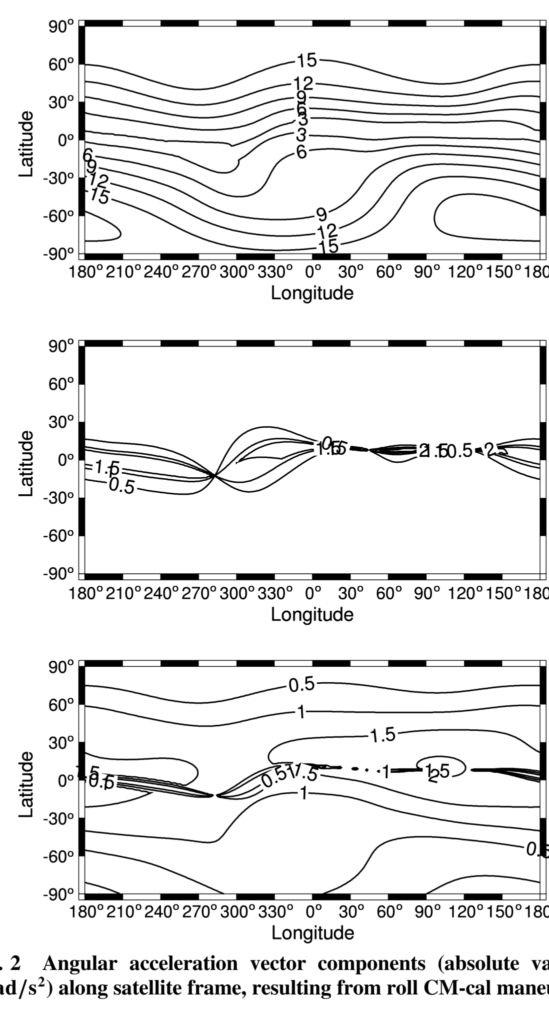

Fig. 2 Angular acceleration vector components (absolute value in $\mu\mathrm{rad/s}^2$) along satellite frame, resulting from roll CM-cal maneuver.

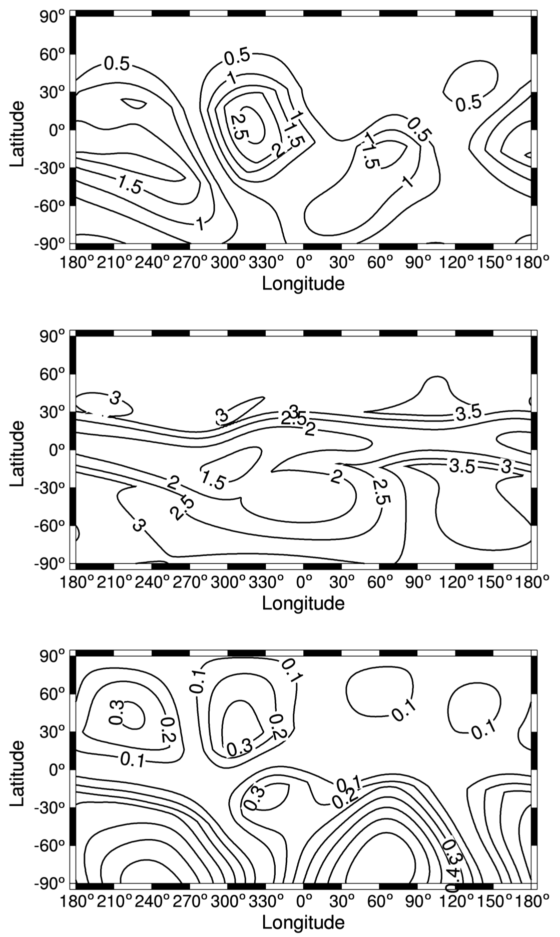

Fig. 3 Angular acceleration vector components (absolute value in $\mu \mathbf{rad/s^2}$) along satellite frame, resulting from pitch CM-cal maneuver.

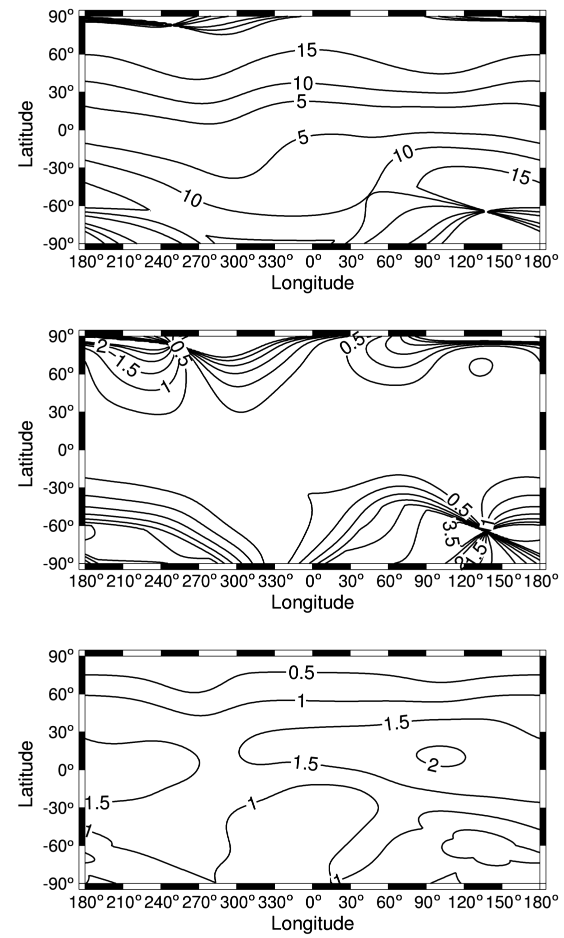

Fig. 4 Angular acceleration vector components (absolute value in $\mu \mathbf{rad/s^2}$) along satellite frame, resulting from yaw CM-cal maneuver.

twangs occur in the sunlight. The data segments during a CM-cal maneuver with a preponderance of twangs have to be discarded in the processing. Thus, a careful choice of the maneuver location results in more twang-free data for analysis.

The twangs are identifiable in the data using empirical criteria for signal change over short durations [8]. For the purposes of planning the CM-cal maneuver, the daily, weekly, and long-term statistics of twang locations and intensity are monitored on an ongoing basis by the GRACE operations team, using GRACE accelerometer data. Shortly before a planned CM-cal maneuver campaign, the recent geographical distribution trends of twangs are analyzed and a recommendation is made for the geographic placement of the CM-cal maneuvers.

The third consideration is to place the CM-cal maneuvers, preferably in the northern hemisphere, since the GRACE ground monitoring stations are located in Weilheim, Germany. This choice is facilitated by the realization that the angular acceleration amplitudes are roughly symmetric about the equator. Based on these considerations, the past several CM-cal campaigns have been located as follows. Near the equator, yaw maneuver was within a latitude range of10 to 20°N and longitude range of 80 to 140°, and pitch maneuver was within a latitude range 10 to 20°N and longitude range of 305 to 325°. Near the pole, roll and pitch maneuvers were at a latitude range of 60 to 80°N and at any longitude. All of these maneuvers were carried out in sunlight.

III. Data Analysis

A. Measurement Model

Expressions (1) and (2) can be adapted within the framework of the CM-cal maneuver design to obtain a mathematical model for regression between the linear and angular accelerations in order to estimate the CM-offset vector. We have discussed in the previous section why the first and third terms in Eq. (1) can be ignored, why the seventh (last) term is absent, and why the fifth and sixth terms are slowly changing over the span of CM-cal maneuver.

Turning now to Eq. (2), the SuperSTAR accelerometer output is also scaled and biased and has additive noise relative to the input excitation. The nominal instrument scale factor is designed to be 1.0, though experience with accelerometer scale-factor determination together with GRACE orbits and gravity fields suggests that the true scale factor may be within 2–4% of this value. For the purposes of our modeling, the scale is set equal to 1.0. Not much is known about the SuperSTAR instrument drifts at time scales of a few hundred seconds, except that these must be slowly changing as well [8]. The accelerometer noise is specified in Table 2. Analysis of GRACE data during quiet periods [9] suggests that the accelerometer is close to performing at the specified levels.

Based on these arguments, during the CM-cal maneuver, the acceleration observation can be modeled as

$$\mathbf{A}_{\text{out}} = -\dot{\boldsymbol{\omega}} \times \mathbf{d} - \boldsymbol{\omega} \times (\boldsymbol{\omega} \times \mathbf{d}) + \boldsymbol{\alpha} t + \boldsymbol{\beta} + \boldsymbol{\eta} \tag{4}$$

where $\mathbf{d}$, $\boldsymbol{\alpha}$, and $\boldsymbol{\beta}$ are the vector unknowns; $\mathbf{A}_{\text{out}}$ and $\dot{\boldsymbol{\omega}}$ are the linear and angular acceleration data output from the accelerometer; and $\boldsymbol{\eta}$ stands for a combination of measurement errors and residual mismodeled or ignored terms.

B. Determination of Angular Velocity

The regression model in Eq. (4) requires the knowledge of the angular velocity of the satellite. This information is derived from use of GRACE star-camera data. The GRACE star-camera instrument consists of two separate perpendicularly mounted sensor heads. Each sensor head has a 22×16 deg field of view. The sensor head images

Table 2 GRACE SuperSTAR accelerometer performance characteristics

Accelerometer	
Scale factor	$1.0 \pm 1\%$ for all axes (estimates show <0.2% scatter in X direction and approximately 2–4% in Y and Z directions)
Bias	<2 μm/s^2 in each direction (generally known to be constant over the duration of a maneuver campaign)
Instrument noise power spectral density	
Roll and yaw axes	$\mathrm{PSD}(f) < (1 + \frac{0.005}{f}) \times 10^{-20}$ m^2 s^{-4} Hz^{-1}
Pitch axis	$\mathrm{PSD}(f) < (1 + \frac{0.1}{f}) \times 10^{-18}$ m^2 s^{-4} Hz^{-1}

are routed to the data processing unit, which compares a constellation of up to 70 stars with a reference star catalog. A successful match leads to a three-axis attitude quaternion solution [3]. Both star cameras onboard GRACE output the quaternion observation data every 1 s.

During a CM-cal maneuver, in the absence of attitude thruster activations, the applied periodic magnetic torques will dominate over the environmental torques. Therefore, in this short duration, the satellite attitude dynamics can be well modeled by

$$\dot{\mathbf{q}}(t) = \tfrac{1}{2}\Omega(\boldsymbol{\omega})\mathbf{q}(t) \tag{5}$$

$$\dot{\boldsymbol{\omega}}(t) = J^{-1}(\mathbf{m} \times \mathbf{B} - \boldsymbol{\omega} \times (J\boldsymbol{\omega})) \tag{6}$$

where J is the moment-of-inertia tensor with respect to the CM of the spacecraft and

$$\Omega(\boldsymbol{\omega}) = \begin{bmatrix} 0 & \boldsymbol{\omega}_z & -\boldsymbol{\omega}_y & \boldsymbol{\omega}_x \\ -\boldsymbol{\omega}_z & 0 & \boldsymbol{\omega}_x & \boldsymbol{\omega}_y \\ \boldsymbol{\omega}_y & -\boldsymbol{\omega}_x & 0 & \boldsymbol{\omega}_z \\ -\boldsymbol{\omega}_x & -\boldsymbol{\omega}_y & -\boldsymbol{\omega}_z & 0 \end{bmatrix} \tag{7}$$

The quaternions from the GRACE star cameras are the direct, and noisy, observations of the quaternion state of this dynamical system. The moments and products of inertia for the satellite were measured during ground balancing of the satellites and made available through GRACE project documents.

Equations (5–7) form a standard nonlinear dynamic estimation system. The estimated parameter vector can be defined as $X(t) = [\mathbf{q}(t), \boldsymbol{\omega}(t)]^T$ and thereby its corresponding state residual is $x(t) = [\Delta\mathbf{q}(t), \Delta\boldsymbol{\omega}(t)]^T$. One can obtain the partial derivatives of Eqs. (5) and (6) with respect to the state to linearize the system. Then the state transition matrix $\Phi(t_k, t_0)$ for propagating the state residual and the observation-state mapping matrix $\tilde{H}(t_k)$ can be obtained for any given time epoch t_k. The minimum variance estimate $\hat{x}(t_0)$ for the initial conditions of the above system can then be used to update the a priori estimate of the system state $X^*(t_0)$. Numerical integration of the dynamical system with this updated initial state gives $\mathbf{q}(t)$ and $\boldsymbol{\omega}(t)$ at any time t. Complete details of this procedure are presented in [7].

C. Data Adjustment Procedure

For each CM-cal maneuver campaign, all available twang-free spans of linear and angular acceleration data are combined in a least-squares adjustment of CM-offset and other parameters. The linear acceleration measurements are also low-pass-filtered with a cut frequency of two times the CM-cal oscillation frequency of 0.083 Hz, in order to remove the high-frequency noise before the data are used in processing.

The data processing is carried out in two steps. First, a linear trend and bias are removed from the low-pass-filtered accelerometer data. In preparation for the second step, new accelerometer data residuals are calculated as

$$\mathbf{y}_i = \mathbf{A}_{\mathrm{out}} - \boldsymbol{\alpha} t_i - \boldsymbol{\beta} \tag{8}$$

From these new residuals, in the second step, the CM-offset $\mathbf{d}$ can be estimated. The observation-state mapping matrix at any epoch t_i is denoted by H_i and given by

$$H_i = \begin{bmatrix} \boldsymbol{\omega}_y^2 + \boldsymbol{\omega}_z^2 & -\boldsymbol{\omega}_x\boldsymbol{\omega}_y + \dot{\boldsymbol{\omega}}_z & -\boldsymbol{\omega}_x\boldsymbol{\omega}_z - \dot{\boldsymbol{\omega}}_y \\ -\boldsymbol{\omega}_x\boldsymbol{\omega}_y - \dot{\boldsymbol{\omega}}_z & \boldsymbol{\omega}_x^2 + \boldsymbol{\omega}_z^2 & -\boldsymbol{\omega}_z\boldsymbol{\omega}_y + \dot{\boldsymbol{\omega}}_x \\ -\boldsymbol{\omega}_x\boldsymbol{\omega}_z + \dot{\boldsymbol{\omega}}_y & -\boldsymbol{\omega}_z\boldsymbol{\omega}_y - \dot{\boldsymbol{\omega}}_x & \boldsymbol{\omega}_y^2 + \boldsymbol{\omega}_x^2 \end{bmatrix} \tag{9}$$

In Eq. (9), $\dot{\boldsymbol{\omega}}$ is known from the accelerometer measurements and $\boldsymbol{\omega}(t)$ is determined from star-camera measurements. The data from a complete CM-cal campaign are separated into n individual clean (twang-free) data segments, from which a unified estimate of the CM-offset vector is obtained as

$$\mathbf{d} = \left(\sum_{i=1}^{n} H_i^T R^{-1} H_i\right)^{-1} \left(\sum_{i=1}^{n} H_i^T R^{-1} y_i\right) \tag{10}$$

where $\mathbf{d}$ is the CM-offset vector, i is the index of a clean-data segment, n is the total number of clean-data segments from that campaign, and R is the observation weight matrix. An alternate approach is to simultaneously estimate the linear trend and bias together with the CM-offset. The two methods were found to give the same estimates to within 10 μm for the CM-offset, and hence the two-step process was used thereafter. In this approach, no attempt was made to give different weight to measurements at different epochs. To acknowledge the higher errors in one accelerometer measurement axis, the data for the data in the pitch axis (Table 2) were assigned a weight of 1.0, and the roll and yaw axes were assigned a weight of 10.0 in the units of the observations. This choice leads to an error covariance estimate for the CM-offset that is uncalibrated in an absolute sense, which is acceptable since these error estimates are not derived from the formal statistics but are estimated using independent means in this paper.

Equation (8) [and also Eq. (1)] illustrates the intuitively obvious fact that a large angular acceleration in one direction will induce a large linear acceleration signal in the two orthogonal directions. In addition, since the angular accelerations in this case are generally larger than the product of the angular velocities, we may also use Eq. (9) to show that the variance of the CM-offset estimate along each axis is approximately proportional to the square of the angular acceleration in that direction. This suggests that the CM-offset in the direction of the largest angular acceleration will be the least well determined. As described in Sec. II.B, the X component of angular acceleration is about 10 times larger than the Y and Z components, and thus it is expected that GRACE CM-cal analysis gives better estimates along the pitch and yaw axes than along the roll axis. Alternative strategies for optimizing the determination of the CM-offset in all directions have been discussed in [7].

D. Results

Since the GRACE satellites were launched, CM-cal campaigns have been carried out 16 times for GRACE A and 15 times for GRACE B, as of October 2008. The CM-offset has been trimmed four times for GRACE A and three times for GRACE B. The CM-offset has been held within the 100 μm requirements since the first CM-trim for GRACE B and second CM-trim for GRACE A, which took place very early in the mission.

If the CM-offset is large, it is expected that a periodic signal in the linear acceleration at the same frequency as the angular acceleration will be more evident than when the offset is small. This was particularly so in the early mission, before the first CM-trim. An illustrative example is the roll maneuver of GRACE B carried out on 3 April 2002. Figure 5 shows the linear acceleration observations and low-pass-filtering of this data along the y axis, the product of the CM-offset estimate along the z axis, and the angular accelerations along the x axis. The figure clearly shows the match of the linear and angular accelerations along the pitch axis due to the large offset along the yaw axis and the large angular acceleration along the roll axis with a magnitude of 18 $\mu\mathrm{rad/s^2}$. This maneuver campaign gave a CM-offset estimate of -21, -18, and 202 μm.

Another illustrative example of CM-cal maneuver, this time with a smaller offset, is the most recent one carried out on 3 September 2008, consisting of seven maneuvers. There were two yaw maneuvers and one pitch maneuver near the equator (at latitude 20°N) and two pitch maneuvers and two roll maneuvers near the polar regions (at latitude 60°N). These maneuvers were all carried out when the satellites were in sunlight.

The data from one of the yaw maneuvers for GRACE A are shown in Fig. 6, as an example. Note that the Y-axis scale in Fig. 6 is one-fourth that of Fig. 5. This maneuver was executed at a latitude of 20° and longitude of 118°. The commanded torque $\mathbf{T}_e$ is the product of $[1 \quad 0 \quad 0]^T$ N · m and a square waveform function with a period of 12 s. This maneuver lasted 180 s. Because of a very small CM-offset along each axis, unlike in Fig. 5, although the noise levels are the same as before, the signal in the linear acceleration is much smaller.

The GRACE A accelerometer data generally has fewer occurrences of twangs than does GRACE B. The typical percentages of clean-data segments are 32 and 25% for GRACE A and B, respectively. The estimates of CM-offsets, determined from CM-cal maneuvers during the mission, are listed in Table 3. This table also shows the dates on which the CM-offset was trimmed and the amounts by which it was trimmed.

IV. Validation of Results

We have used two approaches to validate the estimates of CM-offsets from the CM-cal maneuver data analysis and to calibrate the error bounds on these estimates. The first uses a comparison of estimates against an independent CM-offset estimate in the X direction, and the second uses tests of internal consistency using withheld data sets.

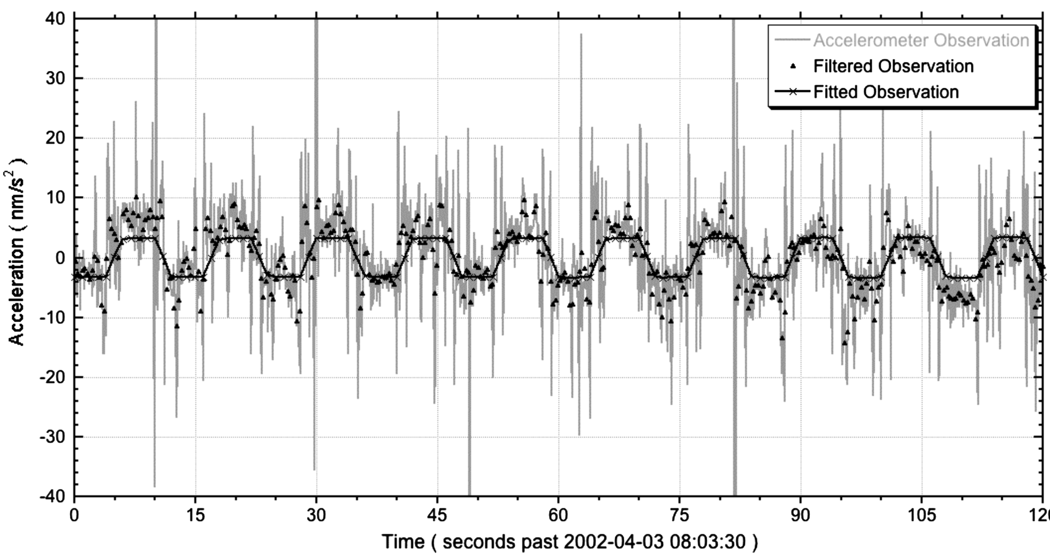

Fig. 5 Raw, filtered, and fitted linear accelerations from an early-mission CM-cal maneuver.

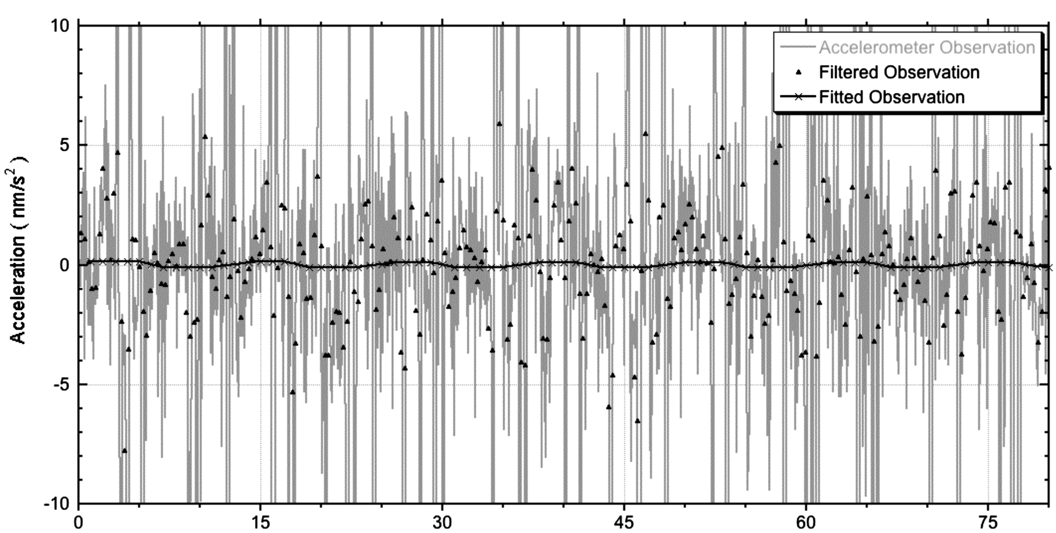

Fig. 6 Raw, filtered, and fitted linear accelerations from a recent CM-cal.

Table 3 List of CM-cal maneuvers and CM-trim events during the GRACE mission

Date	GRACE A, μm	GRACE B, μm
3 April 2002	——	−21 −18 202
4 April 2002	−256 127 −118	——
15 April 2002	−268 133 −117	11 −12 195
25 April 2002	——	−17 4 210
29 April 2002	−236 138 −121	——
6 May 2002	CM-trim (237 −127 116)	CM-trim (0 0 −203)
7 May 2002	−150 −2 −15	−38 −15 −35
4 Feb. 2003	——	20 12 45
27 Feb. 2003	−170 33 −52	——
7 March 2003	CM-trim (161 −30 40) 31 −38 13	——
3 Dec. 2003	50 −22 53	14 −19 66
29 Jan. 2004	66 1 −15	13 34 6
8 Sept. 2004	17 −29 27	6 61 40
1 Dec. 2004	76 −30 59	32 10 19
10 May 2005	CM-trim (−98 0 0)	CM-trim (−82 0 0)
11 May 2005	−14 −30 37	3 17 27
23 Feb. 2006	20 −19 53	3 37 30
17 Oct. 2006	20 −62 56	−18 23 13
12 April 2007	CM-trim (−46 26 −41)	CM-trim (−75 −24 −24)
4 June 2007	−40 10 33	−37 −6 7
4 Feb. 2008	16 2 −5	6 3 −2
3 Sept. 2008	−7 −9 17	5 23 31

A. External Validation

As has been noted earlier, since GRACE has no moving parts other than the CM-trim mechanism, the only cause for a change in the CM-offset is the differential consumption of fuel from the two GN2 tanks (Fig. 1). Each tank can be modeled as a point mass, located at a fixed distance from the origin of the accelerometer proof mass, but whose mass can change over time. The line joining the two tank masses is assumed to pass through the proof-mass origin and is assumed to be parallel to the satellite X axis. In this manner, differential fuel consumption gives rise to a CM-offset in only the satellite X direction.

Although the absolute value of the CM-offset cannot be known due to limitations in precision of prelaunch measurements, it is possible to track the changes in flight. The initial CM-offset value was assumed to be identically equal to the outcome of the first CM-cal campaign. Since that time, the change in the CM-offset in the X direction has been tracked using estimates of mass remaining in the gas tanks. These gas-tank mass estimates are derived using a *tracking model*, which is an optimal combination of two methods: the *observation method*, which is good over the long durations (months), and the *bookkeeping method*, which is good over the short duration (days to weeks).

The observation method uses a combination of ground and onboard measurements together with equations of state to predict the

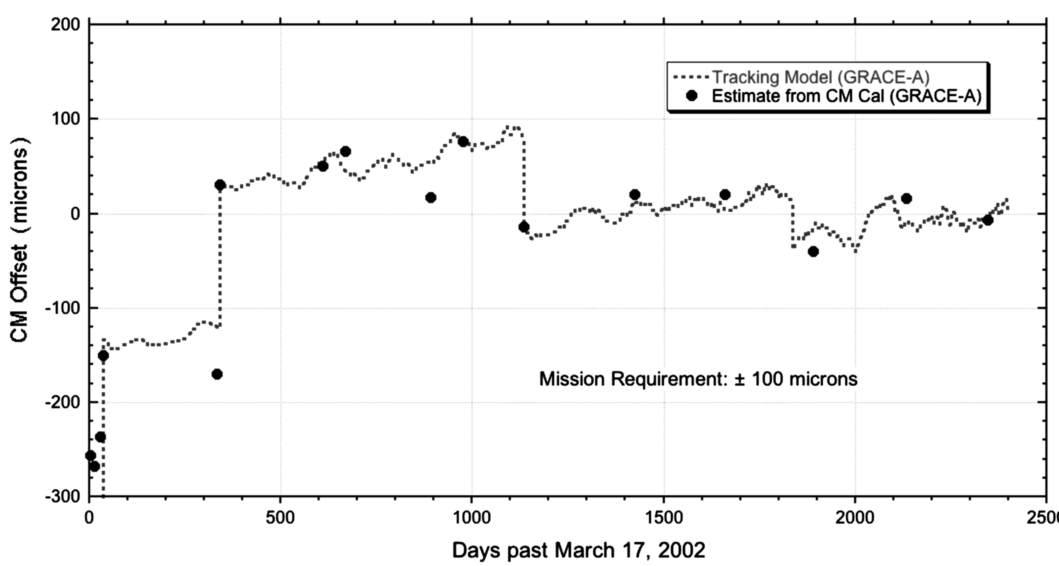

Fig. 7 GRACE A CM-offset estimates in the X direction.

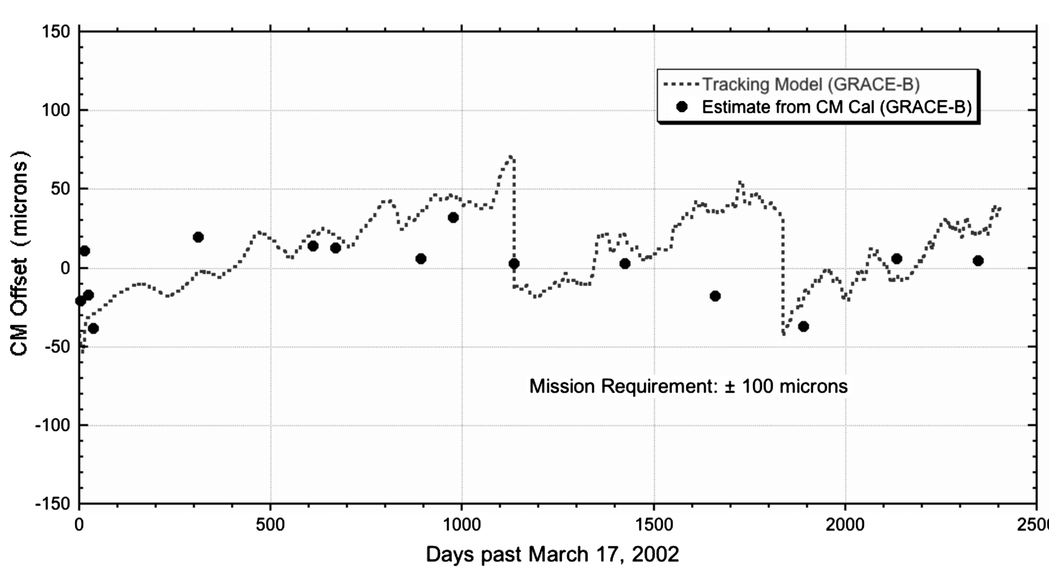

Fig. 8 GRACE B CM-offset estimates in the X direction.

Table 4 Variability of mean values of CM-offset estimates (in microns) for campaign of 3 Sept. 2008 as a function of subset of data used

Axis	Estimates using 100% data	Estimates using 90% data[a]	Estimates using 80% data[a]
		Satellite A	
X	−7	−9.9 (14)	−13 (14)
Y	−9	−10.7 (8)	−10 (6)
Z	17	17.4 (8)	17.4 (14)
		Satellite B	
X	5	8.3 (7)	11.7 (6)
Y	23	18.8 (3)	18.8 (2)
Z	31	33.2 (10)	31.7 (11)

[a]The numbers within parentheses are the scatter (standard deviation) of the estimates about their mean values.

mass of gas in each tank.¶ The variation of tank volume with pressure is known from the manufacturer. Onboard telemetry is available for the pressure and temperature of each tank. The composition of the GN2 fuel is also known from the manufacturer. The cubic equation of state is solved for the molar volume (and thus the density) of the gas for the given measurements of pressure and temperature. This density, together with the tank volume, gives the mass of the gas. The accuracy of this estimate is limited by the low accuracy of the tank pressure and temperature measurements. As a result, small changes such as individual thruster activations cannot be tracked using this method. However, effects of accumulated gas consumption over time can be well observed.

The bookkeeping method, on the other hand, is useful for tracking short-term fuel-consumption trends. GRACE telemetry provides precise information (to millisecond resolution) on the individual attitude thruster activation durations or thruster-on times. The mass-flow rates through the thrusters are only imprecisely known from prelaunch measurements. This deficiency, however, can be made up using a combination method discussed below. Knowledge of mass-flow rates enables a precise calculation of the change in mass over time, though the initial or total value of the mass is not known equally precisely.

The tracking model takes advantage of both the short-term accuracy of the bookkeeping method and the long-term stability of the observation method by computing the CM-offset as an optimal combination of the two results. A sequential Kalman filter is used for this purpose. The state of this filter has seven variables for each satellite: the CM-offset in the X direction, together with six differential mass-flow rates, one for each attitude thruster pair. The system dynamics are modeled as random walk, with a long time constant. The mass estimates from the observation method are used as observations into this system. The thruster-on times are the partial derivatives of the mass estimates relative to the mass-flow rates. This combination method has the advantage of being insensitive to common errors in gas-mass calculations.

The history of CM-offset along the X axis is presented in Figs. 7 and 8 for GRACE A and GRACE B, respectively. The continuous lines are the estimates from the tracking model, and the points denote the results from analysis of CM-cal maneuver (presented in Table 3). In general, good agreement is seen between the tracking model calculation and the CM-cal results. The tracking model result also shows oscillations on the order of 180 days or so. This is believed to be related to the drift in the temperature and pressure sensors with the changing solar illumination of the satellite.

The rms differences along the X axis between the tracking model and CM-cal results are 21 μm for GRACE A and 22 μm for GRACE B. There are no comparisons along the Y and Z axes, since the tracking model only gives the X component of CM-offset. However, it is expected that the estimation accuracy is better for these two axes, for reasons discussed at the end of Sec. III.C.

¶Private communication with M. Schelkle, 2002.

B. Internal Consistency Tests

Because of the incidence of twangs and spikes in the linear acceleration measurements, approximately 30% of the total data from each CM-cal campaign are used in making an estimate for the CM-offset. To assess the stability of results, we have studied the sensitivity of the estimates with respect to the selection of good data. With the CM-cal on 3 September 2008 as an example, we estimated the CM-offset using 100, 90, and 80% of the total good data. Several subsets of 90 or 80% data could be selected, and the CM-offset was estimated for each subset. Table 4 summarizes the average and the scatter of the CM-offset estimates for each such selection.

The maximum deviations from the mean were 38, 23, and 22 μm along the X, Y, and Z axes, respectively. Together with the results of comparison between the tracking model and CM-cal results in Sec. IV.A, we therefore believe that the CM-offset estimates from CM-cal have, conservatively, an error upper bound of approximately 40 μm along the X axis and 25 μm along the Y and Z axes.

V. Conclusions

The GRACE CM-offsets have been successfully measured and controlled to within 100 μm requirements during its mission lifetime. The CM-offset estimation accuracy from CM-cal is better than 40 μm along the X axis and 25 μm along the Y and Z axes. The results from CM-cal maneuvers have been validated against the results of a tracking model. To date, four CM-trims for GRACE A and three trims for GRACE B have been performed when this offset was out of the range of requirements. The follow-up calibration shows that trims have driven the CM-offset back within requirements. This has ensured collection of high-quality measurements of nongravitational accelerations, free from spurious influences due to rotational or gravity-gradient accelerations.

Acknowledgments

The success of this effort is the result of hard work and cooperation between several members of the Gravity Recovery and Climate Experiment (GRACE) teams in the United States and Germany. The close cooperation between the GRACE Science Data System (responsible for the maneuver design and data analysis) and the mission operations team at German Space Operations Center (GSOC, who perform the center-of-mass calibration) in Oberpfaffenhofen, Germany, is especially acknowledged. The GRACE teams at the Jet Propulsion Laboratory, California Institute of Technology, and at the University of Texas at Austin's Center for Space Research (UTCSR) provided additional support in this work.

References

[1] Tapley, B. D., Bettadpur, S., Ries, J., Thompson, P., and Watkins, M., "GRACE Measurements of Mass Variability in the Earth System," *Science*, Vol. 305, July 2004, pp. 503–505. doi:10.1126/science.1099192

[2] Tapley, B. D., Bettadpur, S., Watkins, M., and Reigber, C., "The Gravity Recovery and Climate Experiment: Mission Overview and Early Results," *Geophysical Research Letters*, Vol. 31, No. 9, May 2004, L09607. doi:10.1029/2004GL019920

[3] Dunn, C., Bertiger, W., Bar-Sever, Y., Desai, S., Haines, B., Kuang, D., et al, "Instrument of GRACE: GPS Augments Gravity Measurements," *GPS World*, Vol. 14, No. 2, Feb. 2003.

[4] Touboul, P., Foulon, B., Rodrigues, M., and Marque J.-P., "In Orbit Nano-G Measurements, Lessons for Future Space Missions," *Aerospace Science and Technology*, Vol. 8, 2004, pp. 431–441. doi:10.1016/j.ast.2004.01.006

[5] Romans, L., "A Note on GRACE CG Offset Determination with Magnetic Torquers," Jet Propulsion Lab., California Inst. of Technology, Rept. D-61014, Pasadena, CA, 2001.

[6] Herman, J., Presti, D., Codazzi, A., and Belle, C., "Attitude Control for GRACE: The First Low-Flying Satellite Formation," *Proceedings of the 18th International Symposium on Space Flight Dynamics*, edited by O. Montenbruck and B. Battrick, ESA SP-548, Noordwijk, The Netherlands, Oct. 2004.

[7] Wang, F., "Study on Center of Mass Calibration and *K*-band Ranging System Calibration of the GRACE Mission," Ph.D. Dissertation, Department of Aerospace Engineering and Engineering Mechanics, Univ. of Texas at Austin, Austin, TX, 2003.

[8] Hudson, D., "In-Flight Characterization and Calibration of the SuperSTAR Accelerometer," M.S. Thesis, Univ. of Texas at Austin, Austin, TX, 2003.

[9] Flury, J., Bettadpur, S., and Tapley, B., "Precise Accelerometry Onboard the GRACE Gravity Field Satellite Mission," *Advances in Space Research*, Vol. 42, No. 8, 2008, pp. 1414–1423. doi:10.1016/j.asr.2008.05.004

D. Spencer
Associate Editor